ISSN (Print) 1226-1750
ISSN (Online) 2233-6656
Journal of Magnetics 28(4), 432-437 (2023) https://doi.org/10.4283/JMAG.2023.28.4.432

Research on Change Factors for Accurate Autocontouring of Organs when RTPs

Jeong-Ho Kim[1], Man-Seok Han[2]*, Min-Cheol Jeon[3]*, and Se-Jong Yoo[4]

[1]Dept. of Radiological Science, Sunlin University, Pohang 37560, Republic of Korea
[2]Dept. of Radiological Science, Kangwon National University, Samcheok 25913, Republic of Korea
[3]Dept. of Radiological Science, Daejeon Health Institute of Technology, Daejeon 34504, Republic of Korea
[4]Dept. of Radiological Science, Konyang University, Daejeon 35365, Republic of Korea

(Received 16 October 2023, Received in final form 29 November 2023, Accepted 5 December 2023)

When planning treatment using Radiation Treatment Planning system (RTPs), errors in the contouring process, which is the pre-planning stage, reduce the accuracy of the treatment. Therefore, we wanted to evaluate the error rate of RTPs, Window Width (WW), Window Level (WL), Hounsfield Unit (HU) values at the set point, and the error rate by organ, which are the causes of errors in the contouring process. The results showed that the error rate of WW, WL and HU of certain areas decreased over time. There were no significant changes in the other variables. Therefore, when performing auto-contouring for each organ, appropriate WW, WL and HU values should be set and additional manual contouring should be performed to ensure the accuracy of the treatment plan.

Keywords : electro-magnetic radiation treatment planning, electro-magnetic radiation therapy, auto-contouring

1. Introduction

Radiation treatment planning systems (RTPs) have significantly evolved since their introduction in the late 19th century [1]. Prior to the implementation of RTPs, dose calculations were performed crudely, resulting in an inability to assess the dose to individual internal organs [2]. Nevertheless, the advancement of measurement technology and medical devices has enhanced the precision and efficacy of radiation therapy [3]. The initial use of contour frames to measure and distribute internal radiation in radiation treatment planning (RTP) increased stability but also emerged as a source of various complications for patients [4, 5]. In particular, it was not feasible to use a three-dimensional human body contouring frame, despite the application of a human body contouring frame. This is due to the application of the transverse axis plane, which corresponds to the centerline velocity in the long axis direction, rather than the long axis direction of the human body [6]. Additionally, creating a human body contouring frame with lead ropes and plaster bandages did not allow for consideration of the elasticity of the human body, which resulted in errors by the operator [7]. While the first RTPs made significant strides in acquiring dose distribution during radiotherapy, their accuracy failed to meet expectations [8]. However, the rapid advancement of computers since the Third Industrial Revolution has enabled quick calculations of complex formulas. Additionally, the development of computed tomography (CT) allows for obtaining precise images in a short timeframe, leading to the feasibility of the current RTPs [9]. Current treatment planning systems precisely calculate radiation dose by converting three-dimensional contours of patient and internal organs using CT imaging and radiation attenuation coefficients. This enables monitoring of both tumor and normal organ dose distribution during radiation therapy. [10] Additionally, the implementation of inverse planning has facilitated the acquisition of personalized radiation dose distributions, leading to significant variations in radiotherapy survival rates [11, 12]. Despite the utilization of precise and individualized RTPs, disparities persist due to diverse user abilities [13]. Variability among users arises from fundamental parameters, such as optimization in inverse planning [14]. However, improving the user's competence to a certain level is achievable due to established

*Co-Corresponding author: Tel: +82-42-670-9179
Fax: +82-42-670-9570, e-mail: 99jmc@hanmail.net
Tel: +82-33-540-3383, Fax: +82-33-540-3389,
e-mail: angio7896@naver.com

systematic courses and preliminary studies [15, 16]. Discrepancies in radiotherapy plan results can stem not only from the conditions, but also from the preceding stages [17]. The stages can be classified into the acquisition stage of CT images, the transmission stage of images, and the contouring of tumor and normal organs after storing images [18-20]. Especially in cases of contouring errors, it is frequently impossible to verify if errors have arisen even subsequent to the completion of radiotherapy [21]. The process of outlining tumors and normal organs for radiotherapy planning varies among medical institutions. Typically, the doctor in charge performs the outlining of tumors, while the person in charge of radiotherapy planning performs outlining of normal organs [22-24]. The individual responsible for radiation therapy planning is accountable for equipment quality control and planning of radiation therapy. The workload is correlated with the number of patients requiring radiation therapy planning, which can lead to an increased burden of work [25-27]. The number of normal organs that require outlining varies based on the location, number, and size of tumors [28]. Therefore, radiotherapy planners seek a more straightforward technique that maintains precision [29]. In response, RTPs have created and utilized autocontouring tools that are commonly employed by radiotherapy planners [30]. However, when utilizing autocontouring tools, Hounsfield unit (HU) alters the Window Width (WW) and Window Level (WL) conditions at the reference position [31]. Accurate organ contour representation is crucial for precise radiotherapy. To assess the reliability and accuracy of autocontouring, our study aimed to evaluate the tool's accuracy under variable conditions and identify means to enhance its reliability.

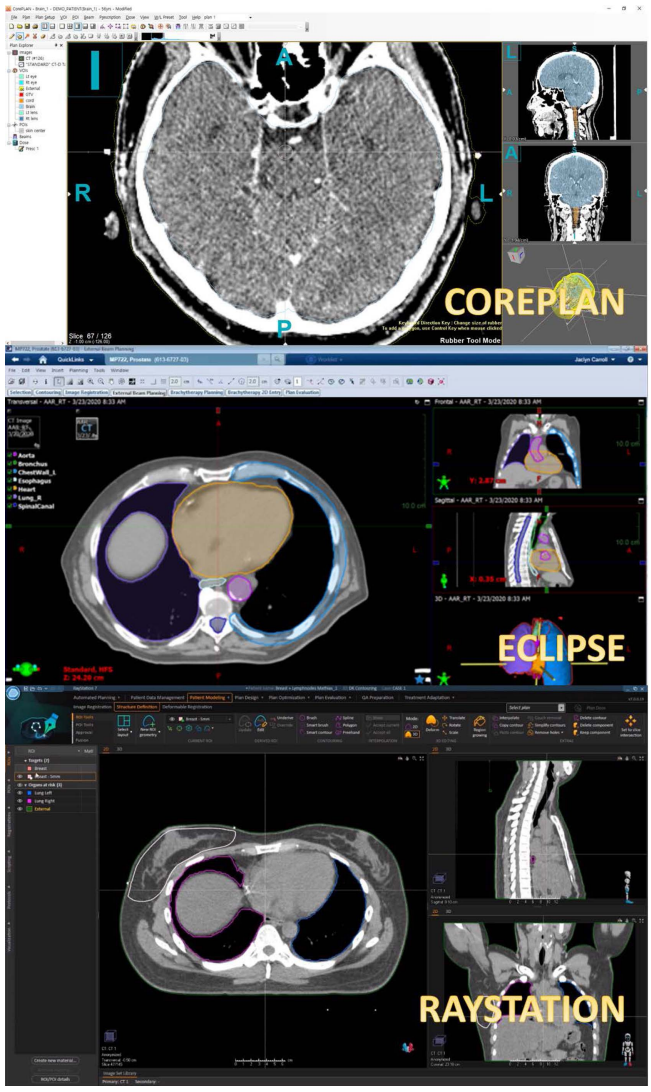

Fig. 1. (Color online) Images of Core-plan, Eclipse, Raystation RTPs.

2. Material and Method

The study focused on three RTPs: Coreplan (Synesol, Korea), Eclipse (Varian, USA), and Raystation (RaySearch Laboratories, Sweden), displayed in Fig. 1. The auto-contouring tool was employed for each RTP, specifically the Brain, Lung, and 6th Lumbar Spine Body, as demonstrated in Fig. 2 of Coreplan. The study's experimental methodology assessed the error rate of automatic contouring results for five variables: type of RTPs, WW, WL, HU value at the reference point, and applied organ. Technical term abbreviations are explained upon first use. The reference volume underwent manual contouring from a 300 % magnification image for standard WW and WL. The RTPs employed were Core-plan, Eclipse, and Raystation. The HU values for WW, WL, and target are tabulated in Table 1. For the WW and WL conditions, the default value varies based on the long term, resulting in WW being divided into 10 sections and WL into 6 sections. Similarly, the range of HU values for the set point varied by organ, thus leading to the division of HU values into low, medium, and high bands. To compare the change in each condition, the error rate of the volume was compared to the reference volume.

3. Result

3.1. Comparison of different RTP types

Error rates for automatic and manual contouring for each RTP are presented in Table 2. Technical abbreviations are defined upon first use. For Core-plan, the error rate varied from 0.4 % to 837.5 % with an average of

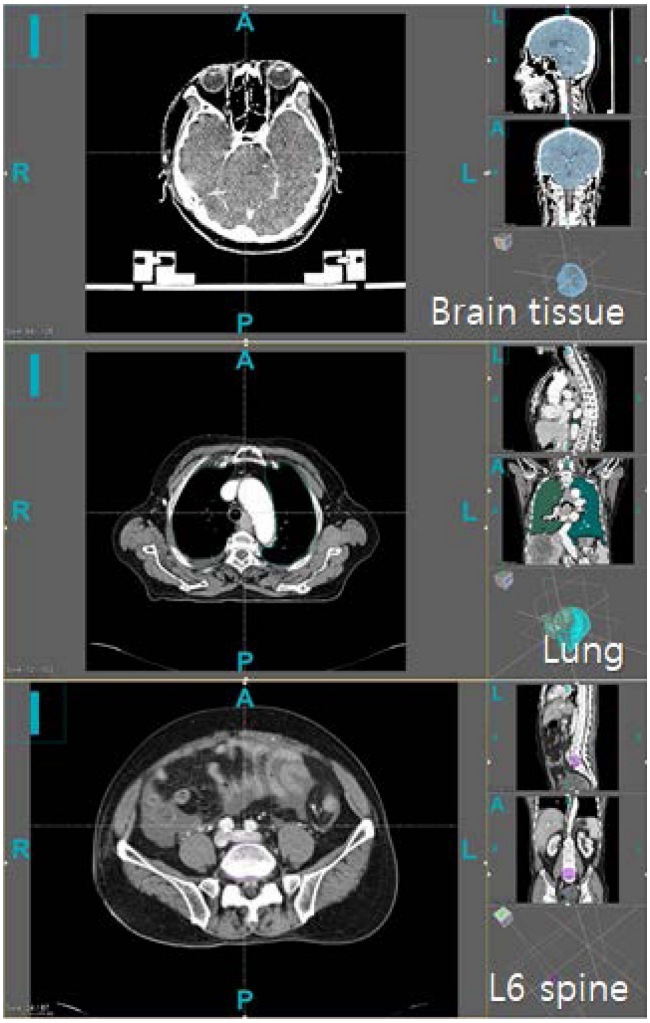

Fig. 2. (Color online) Sample images of the Brain, Lungs, Spine.

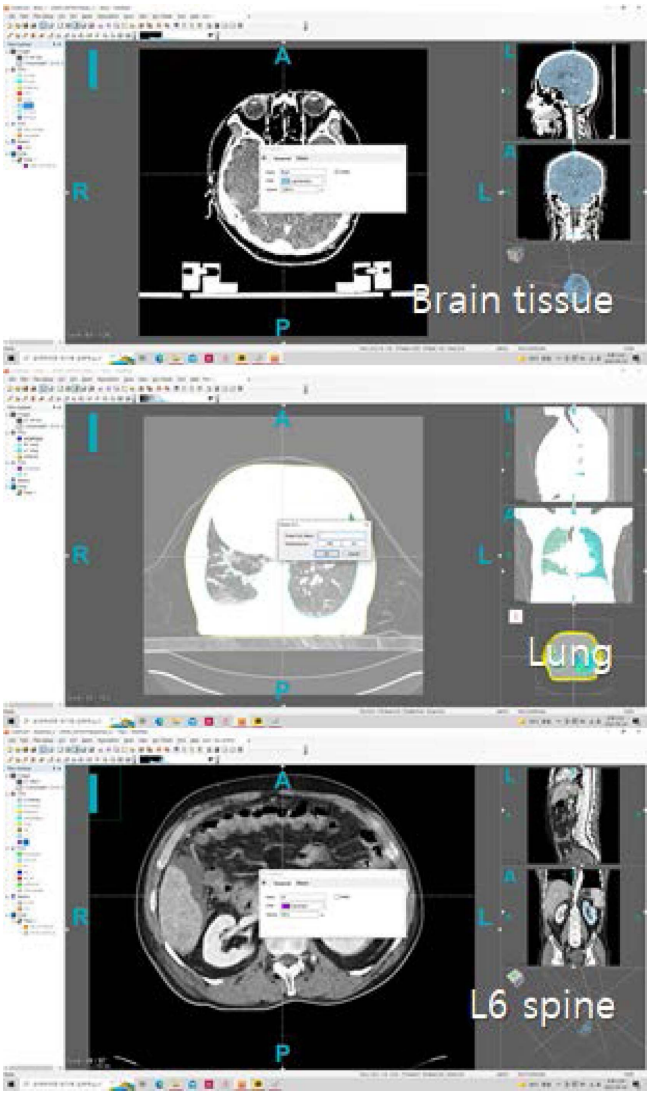

Fig. 3. (Color online) Manual contouring images of the Brain, Lungs, Spine.

Table 2. Error rates for different types of RTPs.

Types of RTPs	Min. error rate	Max. error rate	Aver. error rate
Core-plan	0.40 %	837.50 %	363.63 %
Eclipse	0.19 %	800.60 %	344.57 %
Raystation	0.10 %	913.45 %	360.96 %

363.63 %. For Eclipse, the error rate ranged from 0.19 % to 800.60 % with an average of 344.57 %. Finally, for Raystation, the error rate ranged from 0.1 % to 913.45 %

Table 1. Conditions for WW, WL, and HU values for auto-contouring.

Brain	WW	200, 300, 400, 500, 600, 700, 800, 900, 1000, 1100
	WL	300, 660, 1020, 1380, 1740, 2100
	HU	1000, 1050, 1100
Lung	WW	300, 500, 700, 900, 1100, 1300, 1500, 1700, 1900, 2100
	WL	200, 400, 600, 800, 1000, 1200
	HU	80, 250, 1000
Spine	WW	300, 500, 700, 900, 1100, 1300, 1500, 1700, 1900, 2100
	WL	200, 400, 600, 800, 1000, 1200
	HU	1000, 1100, 1200

with an average of 360.96 %. The discrepancy in the highest error rate is attributable to the entire screen being designated as one zone, as no zone setting exists, precluding the differentiation of various types of RTPs through maximum and average error rates. Notwithstanding, the deviation of error values by Core-plan, Eclipse, and Raystation is insignificant when comparing trends using the minimum error rate.

3.2. Comparison of changes in WW

The auto-contouring error rate was analyzed for each long-term period due to the difference in WW value sets. Table 3 illustrates the results of the minimum error rate based on the change in WW. For brain, the minimum error rate was 0.19 % and the maximum error rate was 850.52 %. Similarly, for lung, the minimum error rate was 0.10 % and the maximum error rate was 229.80 %, while for the spine, the minimum error rate was 97.17 % and the maximum error rate was 882.66 %.

3.3. Comparison of changes in WL

As with the previous method (WW), we evaluated the minimum error rate for each organ in regards to WL. Table 4 presents the error rate results for auto-contouring according to the changes in WL. The minimum error rate for the brain was 0.19 %, and the maximum was 913.45 %. For the lung, the minimum error rate was 0.10 %, and the maximum was 229.80 %, also as observed in WW. For the spine, the minimum error rate was 97.12 %, and the maximum was 882.66 %.

3.4. Comparison by HU of the target value

Table 5 presents the comparison of error values for auto-contouring based on changes in HU values from the set point. The findings indicate that for Brain, the minimum error value is 0.19 % at Low and the maximum

Table 3. Error rate as WW changes.

Part	WW	Min.	Max.	Aver.	Part	WW	Min.	Max.	Aver.
Brain	200	43.60 %	59.80 %	53.50 %	Lung	1300	12.16 %	200.90 %	64.90 %
	300	43.60 %	59.80 %	53.50 %		1500	13.16 %	200.90 %	64.67 %
	400	43.60 %	59.80 %	53.50 %		1700	12.73 %	100.00 %	52.95 %
	500	1.57 %	36.02 %	18.60 %		1900	15.21 %	100.00 %	52.88 %
	600	0.19 %	15.29 %	4.94 %		2100	3.90 %	100.00 %	52.56 %
	700	2.58 %	37.10 %	20.86 %	Spine	300	97.17 %	882.66 %	561.99 %
	800	800.62 %	913.45 %	850.52 %		500	97.17 %	824.80 %	546.54 %
	900	800.62 %	913.45 %	850.52 %		700	521.92 %	824.80 %	678.56 %
	1000	800.62 %	913.45 %	850.52 %		900	521.92 %	824.80 %	659.50 %
	1100	800.62 %	913.45 %	850.52 %		1100	521.92 %	824.80 %	635.73 %
Lung	300	0.10 %	229.80 %	104.66 %		1300	521.92 %	824.80 %	621.60 %
	500	2.13 %	229.80 %	107.16 %		1500	521.92 %	824.80 %	702.33 %
	700	3.74 %	229.80 %	94.65 %		1700	521.92 %	824.80 %	626.35 %
	900	3.26 %	204.80 %	63.83 %		1900	521.92 %	824.80 %	664.32 %
	1100	7.37 %	200.90 %	65.13 %		2100	521.92 %	824.80 %	664.32 %

Table 4. Error rate as WL changes.

Part	WW	Min.	Max.	Aver.	Part	WW	Min.	Max.	Aver.
Brain	300	11.59 %	913.45 %	362.74 %	Lung	800	2.28 %	200.40 %	48.46 %
	660	5.02 %	913.45 %	362.06 %		1000	0.10 %	100.00 %	43.93 %
	1020	1.07 %	913.45 %	359.63 %		1200	3.26 %	229.80 %	98.93 %
	1380	0.37 %	913.45 %	360.24 %	Spine	200	521.92 %	882.66 %	721.98 %
	1740	0.19 %	913.45 %	360.19 %		400	521.92 %	824.80 %	709.94 %
	2100	0.36 %	913.45 %	359.34 %		600	521.92 %	824.80 %	635.73 %
Lung	200	31.88 %	204.80 %	94.55 %		800	521.92 %	824.80 %	647.23 %
	400	17.85 %	204.80 %	87.20 %		1000	97.12 %	824.80 %	550.93 %
	600	3.90 %	200.40 %	60.96 %		1200	97.17 %	824.80 %	550.93 %

Table 5. Error rate as HU value changes.

Part	HU	Min.	Max.	Aver.
Brain	Low	0.19 %	913.45 %	360.33 %
	Middle	0.43 %	913.45 %	362.08 %
	High	1.04 %	913.45 %	359.69 %
Lung	Low	0.38 %	229.80 %	40.70 %
	Middle	0.10 %	229.80 %	40.02 %
	High	100.00 %	229.80 %	136.29 %
Spine	Low	97.21 %	882.66 %	629.03 %
	Middle	97.17 %	882.66 %	650.33 %
	High	97.12 %	882.66 %	629.00 %

error value is 913.45 % at Low, Medium, and High. Similarly, for Lung, the minimum error value is 0.10 % at Middle and the maximum error value is 229.80 % at Low, Medium, and High. For Spine, the minimum error value is 97.12 % for High, and the maximum error value is 882.66 % at Low, Medium, and High.

3.5. Comparison by organ type

Please refer to Table 6 for a breakdown of results by organ type. The minimum and maximum percentages for brain were 0.19 % and 913.45 %, respectively. For lung, the minimum and maximum percentages were 0.10 % and 229.80 %, respectively. The minimum and maximum percentages for spine were 97.12 % and 882.66 %, respectively.

Table 6. Error rate based on part.

Division	Min.	Max.	Aver.
Brain	0.19 %	913.45 %	360.70 %
Lung	0.10 %	229.80 %	72.34 %
Spine	97.12 %	882.66 %	636.12 %

4. Discussion

Radiotherapy has become more precise with the use of CT scans, computerized treatment planning systems, retrospective treatment planning, and fusion imaging. However, the process of acquiring images and calculating accuracy involves manual labor, such as outlining each organ, which can result in accuracy errors. Auto-contouring has been implemented to improve convenience and accuracy in work. However, errors can occur due to various factors affecting the algorithm. To mitigate human

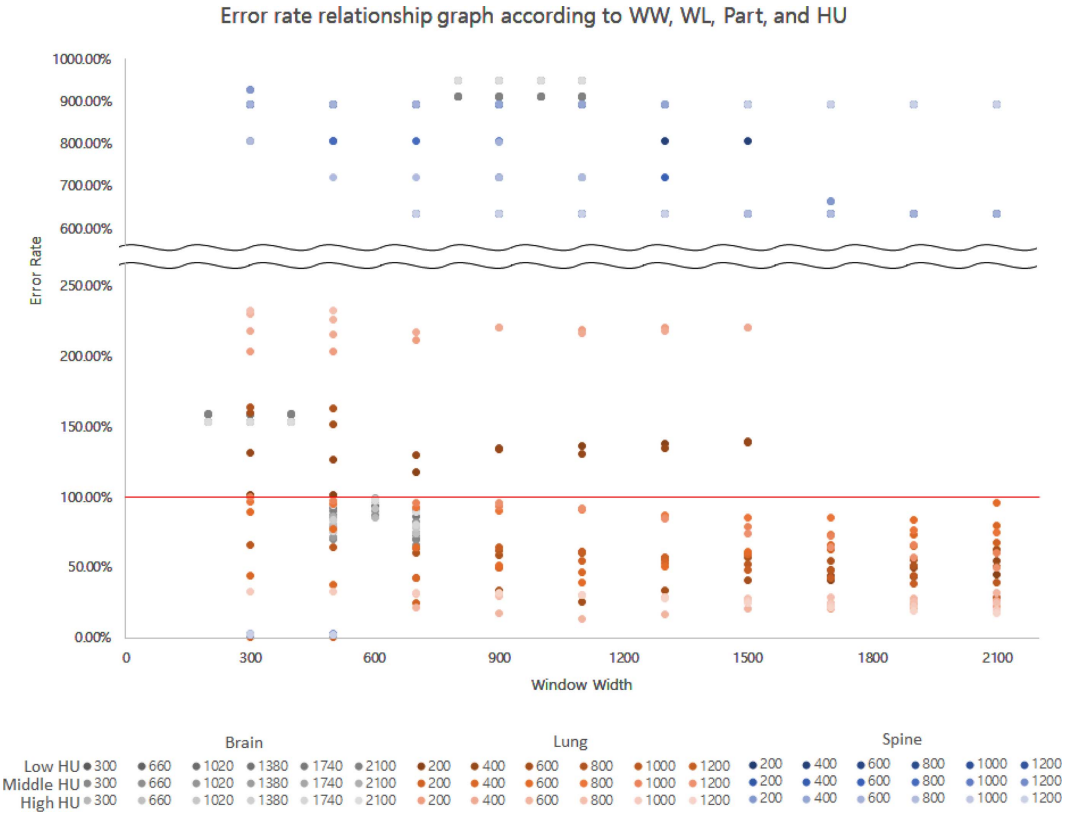

Fig. 4. (Color online) Error rate graph according to change in conditions of change factor.

error, we conducted an analysis of the factors impacting auto-contouring, representing a significant study for precise cancer treatment. However, this study is limited in its ability to make broad generalizations due to the fact that the sample images are embedded in RTPs and only include certain organs, such as the brain, lungs, and spine. Additionally, the values for WW, WL, and HU were not uniformly applied to each organ, thus limiting the ability to accurately trend the results with wide intervals.

5. Conclusion

Auto-contouring is a valuable tool in radiotherapy planning to ensure representation of the most commonly used organs. However, this study suggests the limitations of auto-contouring when using basic WW and WL, particularly for organs with similar HU values to surrounding tissues, such as the spine. In these cases, manual contouring is more appropriate due to the high error rate of auto-contouring. The brain exhibited an error rate within 3 % for WW 600 and WL 1020~2100, demonstrating that auto-contouring is inappropriate for other WWs and WLs with significant error values. For lung, at WW 300 and WL 1000, the error rate was within 1 %. Nevertheless, unlike the brain, lung exhibited a setpoint dependence, with a significant increase in error rate for organs with low HU values when the setpoint HU value was high. Thus, auto-contouring is more effective for organs with high HU values than for neighboring organs. The error rate is lower when the setpoint is closer to the average HU value of each organ. However, the results indicate that the error rate is not 0 %, necessitating additional manual contouring during the treatment planning phase for precise treatment of cancer patients. Instead of solely relying on manual contouring to reduce the workload, we propose implementing a workflow that prioritizes both accuracy and work efficiency. This can be achieved by initially performing auto-contouring for efficient organs and then following up with manual contouring.

References

[1] J. Van Dyk, International Journal of Radiation Oncology* Biology* Physics **71**, 1 (2008).
[2] M. Atiq, Indian Journal of Cancer **54**, 1 (2017).
[3] A. Badnjević, Psychiatria Danubina **33**, 3 (2021).
[4] N. Gennaro, The British Journal of Radiology **93**, 12 (2020).
[5] Y. K. Bae, Scientific Reports **10**, 1 (2020).
[6] R. Mohan, International Journal of Radiation Oncology* Biology* Physics **15**, 2 (1988).
[7] G. C. Bentel, Treatment planning and dose calculation in radiation oncology, Elsevier, New York (2014) pp. 62-72.
[8] T. Hameed, Journal of Applied Clinical Medical Physics **14**, 3 (2013).
[9] D. F. de Carvalho, CBMS **6**, 1 (2018).
[10] A. KILIÇ, Turkish Journal of Medical Sciences **32**, 2 (2002).
[11] M. Ehrgott, OR Spectrum **30**, 1 (2008).
[12] P. L. Robertson, Journal of Neuro-oncology **32**, 1 (1997).
[13] J. Van Dyk, International conference on isotopes in environmental studies, IAEA, Vienna (2006) pp. 210-214.
[14] X. Allen Li, Medical Physics **39**, 3 (2012).
[15] A. J. Olch, Pediatric radiotherapy planning and treatment, CRC Press, London (2013) pp. 25-40.
[16] B. Fraass, Medical physics **25**, 10 (1998).
[17] A. Van Mourik, International Journal of Radiation Oncology* Biology* Physics **79**, 5 (2011).
[18] J. M. Balter, International Journal of Radiation Oncology* Biology* Physics **36**, 1 (1996).
[19] T. F. Lang, Journal of Nuclear Medicine **33**, 10 (1992).
[20] G. A. Ezzell, Medical Physics **23**, 3 (1996).
[21] M. Van Herk, In Seminars in Radiation Oncology **14**, 1 (2004).
[22] V. Chanyavanich, Medical Physics **38**, 5 (2011).
[23] C. Fiorino, Radiotherapy and Oncology **47**, 3 (1998).
[24] H. Zhang, Advances in Radiation Oncology **7**, 6 (2022).
[25] T. J. Netherton, Oncology **99**, 2 (2021).
[26] S. H. Benedict, Medical Physics **35**, 9 (2008).
[27] L. M. Mazur, Practical Radiation Oncology **4**, 2 (2014).
[28] B. E. Nelms, International Journal of Radiation Oncology* Biology* Physics **82**, 1 (2012).
[29] M. V. Sherer, Radiotherapy and Oncology **160**, 1 (2021).
[30] C. Hague, Radiotherapy and Oncology **158**, 1 (2021).
[31] S. P. Primakov, Nature Communications **13**, 1 (2022).